International Journal of Research
Available at https://edupediapublications.org/journals
p-ISSN: 2348-6848
e-ISSN: 2348-795X
Volume 03 Issue 14
October 2016

A Modular Series Connected Converter for a 10 MW Offshore Wind Power Generator Drive with Fuzzy controller

[1] Mr. Pelleti Sivaramaiah,
siva6rise@gmail.com
N.B.K.R. Institute of Science and Technology,
S.P.S.R Nellore, Andhra Pradesh State, India
[2] Smt.Panneerselvam Dhana
Selvi.M.Tech Assistant Professor, dhanaselvi.nbkrist@gmail.com

Abstract:

Medium-voltage power conversion is generally favored for future large wind turbines, e.g., 10 MW, in terms of higher power density, reduced current level, associated losses, and cost of power cables, switchgears, etc. This paper has summarized a fundamental rule to construct multilevel modular high power converters for large wind turbine power conversion. Based on that, three potential multilevel modular high power converter topologies are derived and compared. The topology with a 10-kV generator, a modular power converter, and a multi-winding step-up transformer have been specifically investigated. The large dc-link capacitor (not reliable, high cost, large volume) required in the converter is identified as the key limitation of the system used for wind power conversion. The paper proposes to compensate the ripple power by the grid-side inverter of the multilevel modular converter, thus reducing the dc-link capacitor requirement. The paper has validated the effectiveness of proportional–integral–resonant controller for this purpose. Further, the thermal impact of the proposed ripple power compensation scheme on the converter device junction temperature and the transformer secondary windings has been analytically derived. The paper has also analytically revealed that the proposed ripple power compensation scheme will not affect the grid-side power quality, although there are low-frequency harmonics in the transformer secondary windings. Simulation results with a 10-MW, 10-kV system have validated the proposed converter topology and control strategy with reduced dc-link voltage ripple. Results acquired by simulations with Matlab/Simulink shows that the proposed control algorithm is very flexible and effective under steady and dynamic load conditions

Key Terms- *Permanent Magnet Generators (PMG's), Integrated Gate Commutated Thyristor (IGCT), Voltage Source Inverter (VSI), total harmonic distortion (THD), fuzzy controller, Pulse Width Modulation (PMW)*

1 .Introduction

Today, the most popular large variable-speed wind turbines are rated around 1.5–3 MW. Nevertheless, 7-MW wind turbines have recently appeared and even larger wind turbines, e.g., 10MW, are under development in order to reduce the unit cost of wind power generation. Wind turbines equipped with direct-drive permanent magnet generators (PMGs) and full power converters are generally favored due to simplified drive train structure and thus higher reliability, especially for offshore applications, compared with the doubly fed induction generator-based system. Most of the present wind generator and power converter systems are based on the 690Vand two-level voltage–source or current–source converters are normally used. The continuous increase in wind turbine power ratings will generate larger current, e.g., from 1673 A for 2-MW system to 8810 A for 10-MW system. Power converters are therefore connected in parallel to handle the increasing current. Meanwhile, large current transfer results in a parallel connection of multiple power cables going down through the tower and causes substantial losses, voltage drop, as well as high cost of cables, switchgears, and terminal connections.

These disadvantages can be offset by placing the step-up transformer (e.g., 690 V/33 kV) into the nacelle. However, the bulky and heavy transformer occupies the limited space of the nacelle and increases the mechanical stress of the tower. Therefore, a medium-voltage power conversion system (e.g., 10 kV) would be more desirable for

large wind power conversion by reducing the current level and associated cable cost and losses, as well as improving the system power density. The benefits of adopting medium-voltage power conversion technology have been proved in motor drive applications, where medium-voltage (3–33 kV) configuration is generally used when the system power rating is higher than 1 MW. Table I shows the current rating of an exemplar 5- and 10-MW systems with 690-V and 10-kV voltage level for comparison.

As seen, transferring from low voltage (690 V) to medium voltage (10 kV) can significantly reduce the current level. Further, considering the high maintenance cost and fault-tolerant requirement especially for offshore wind applications, a modular converter and generator structure is even preferable.

Regarding medium-voltage multilevel converter topologies for wind power applications, papers investigate the suitability of three-level neutral-point-clamped converters. Although a higher voltage rating and reduced output harmonics are achieved, the ac-side voltage is limited to 4.0 kV if using 4.5-kV integrated gate-commutated thyristors (IGCTs). The voltage rating may be further increased if using 6-kV IGCT; however, the cost and availability becomes a major concern. A five-level hybrid converter topology with increasing number of devices is presented in to further increase the converter voltage and power capability. However, the reliability restricts its application. If one device fails, the whole converter system operation may be interrupted.

A more applicable way to achieve 6- or 10-kV medium-voltage power conversion is through the cascaded modular converter structure. The voltage level can be easily scaled up by cascading more converter cells. Various Papers have proposed various converter topologies based on this concept. However, the fundamental connections between these topologies are not analyzed. The cascaded converter topology has intrinsic fault-tolerant operation capability. If one cell fails, it can be bypassed and the rest healthy cells can keep operation. One of the main disadvantages of the cascaded converter topology is the large dc-link capacitor required to filter the dc-link voltage ripple from the H-bridge side in each cell. The dc-link capacitor is unreliable and is not favored in wind power applications where maintenance cost is very high. There are no effective solutions to significantly reduce the dc link capacitor. In motor drive applications, diode rectifiers are normally used, which cannot be actively controlled to compensate the ripple power thus reducing the dc-link capacitor.

In this paper, a fundamental rule to construct multilevel modular high power converters for large wind turbine power conversion is proposed. Based on this, three potential multilevel modular wind power converter topologies have been derived using a generalized approach for an exemplar 10-kV, 10e-MW wind turbine. A special focus has been given to the topology comprising a 10-kV generator, a multilevel modular converter, and a multi-winding grid-side transformer.

A solution to reduce the dc-link capacitor is proposed by compensating the ripple power from the three-phase grid-side inverter. A resonant controller is presented to achieve this purpose. The current harmonics induced in the inverter and transformer secondary windings by the proposed control scheme and their impact are also investigated analytically. The converter topology and dc-link capacitor reduction strategy has been simulated and validated with a 10-kV, 10-MW wind power conversion system, where the dc-link voltage ripple is effectively attenuated without affecting the grid power quality.

2. WIND ENERGY

Wind power is the conversion of wind energy into a useful form of energy, such as using wind turbines to make electricity, wind mills for mechanical power, wind pumps for pumping water or drainage, or sails to propel ships. At the end of 2009, worldwide nameplate capacity of wind-powered generators was 159.2 gig watts (GW). Energy production was 340 TWh, which is about 2% of worldwide electricity usage and has doubled in the past three years. Several countries have achieved relatively high levels of wind power penetration (with large governmental subsidies), such as 20% of stationary electricity production in Denmark, 14% in Ireland and Portugal, 11% in Spain, and 8% in Germany in 2009.As of May 2009, 80 countries around the world are using wind power on a commercial basis. Large-scale wind farms are connected to the electric power transmission network; smaller facilities are used to provide electricity to isolated locations. Utility companies increasingly buy back surplus electricity produced by small domestic turbines.

Wind energy, as an alternative to fossil fuels, is plentiful, renewable, widely distributed, clean, and produces no greenhouse gas emissions during operation. However, the construction of wind farms is not universally welcomed because of their visual impact and other effects on the environment. Wind power is non-dispatch able, meaning that for economic operation, all of the available output must be taken when it is available. Other resources, such

as hydropower, and load management techniques must be used to match supply with demand. The intermittency of wind seldom creates problems when using wind power to supply a low proportion of total demand, but as the proportion rises, problems are created such as increased costs, the need to upgrade the grid, and a lowered ability to supplant conventional production. Power management techniques such as exporting excess power to neighboring areas or reducing demand when wind production is low, can mitigate these problems

The Earth is unevenly heated by the sun, such that the poles receive less energy from the sun than the equator; along with this, dry land heats up (and cools down) more quickly than the seas do. The differential heating drives a global atmospheric convection system reaching from the Earth's surface to the stratosphere which acts as a virtual ceiling. Most of the energy stored in these wind movements can be found at high altitudes where continuous wind speeds of over 160 km/h (99 mph) occur. Eventually, the wind energy is converted through friction into diffuse heat throughout the Earth's surface and the atmosphere. The total amount of economically extractable power available from the wind is considerably more than present human power use from all sources.[10] An estimated 72 terawatt (TW) of wind power on the Earth potentially can be commercially viable,[11] compared to about 15 TW average global power consumption from all sources in 2005. Not all the energy of the wind flowing past a given point can be recovered (see Wind energy physics and Betz' law).

2.1 Electricity Generation

In a wind farm, individual turbines are interconnected with a medium voltage (often 34.5 kV), power collection system and communications network. At a substation, this medium-voltage electric current is increased in voltage with a transformer for connection to the high voltage electric power transmission system. The surplus power produced by domestic micro generators can, in some jurisdictions, be fed into the network and sold to the utility company, producing a retail credit for the micro generators' owners to offset their energy costs.

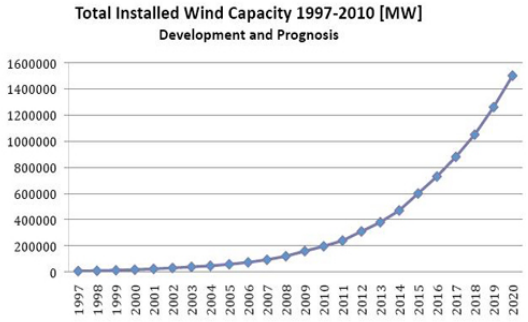

Since wind speed is not constant, a wind farm's annual energy production is never as much as the sum of the generator nameplate ratings multiplied by the total hours in a year. The ratio of actual productivity in a year to this theoretical maximum is called the capacity factor. Typical capacity factors are 20–40%, with values at the upper end of the range in particularly favorable sites.[19] For example, a 1 MW turbine with a capacity factor of 35% will not produce 8,760 MWh in a year (1 × 24 × 365), but only 1 × 0.35 × 24 × 365 = 3,066 MWh, averaging to 0.35 MW.

Online data is available for some locations and the capacity factor can be calculated from the yearly output. Unlike fueled generating plants, the capacity factor is limited by the inherent properties of wind. Capacity factors of other types of power plant are based mostly on fuel cost, with a small amount of downtime for maintenance. Nuclear plants have low incremental fuel cost, and so are run at full output and achieve a 90% capacity factor. Plants with higher fuel cost are throttled back to follow load. Gas turbine plants using natural gas as fuel may be very expensive to operate and may be run only to meet peak power demand. A gas turbine plant may have an annual capacity factor of 5–25% due to relatively high energy production cost. In a 2008 study released by the U.S. Department of Energy's Office of Energy Efficiency and Renewable Energy, the capacity factor achieved by the wind turbine fleet is shown to be increasing as the technology improves. The capacity factor achieved by new wind turbines in 2004 and 2005 reached 36%.

2.2 Wind Expression

Pw is the mechanical power extracted from the airflow [W], D the air density [kg/m3], Cp the performance coefficient or power coefficient, λ the tip speed ratio Vt/Vw, (the ratio between the blade tip speed Vt and the wind speed upstream the rotor Vw [m/s]) Θ the blade pitch angle [deg], and Ar the area swept by the rotor [m2].

$$P_w = \frac{\rho}{2} c_p(\lambda,\theta) A_r v_w^3$$

Cut□in wind speed (in the order of 3□5 m/s) and

• Nominal wind speed or rated wind speed: wind speed at which the nominal power of the turbine is reached (between 11 m/s and 16 m/s)

• Cut□out wind speed: When the wind speed becomes very high, the energy contained in the airflow and the structural loads on the turbine become too high and the turbine is taken out of operation. Depending on whether the wind turbine is optimized for low or high wind speeds, (between 17 and 30 m/s).

• When the wind speed increases to levels above the nominal wind speed, the generated power cannot be increased further, because this would lead to overloading of the generator and/or, if present, the converter. Therefore, the aerodynamic efficiency of the rotor must be reduced, in order to limit the power extracted from the wind to the nominal power of the generating system.

2.3 Power from Wind

Kinetic energy from the wind is used to turn the generator inside the wind turbine to produce electricity. There are several factors that contribute to the efficiency of the wind turbine in extracting the power from the wind. Firstly, the wind speed is one of the important factors in determining how much power can be extracted from the wind. This is because the power produced from the wind turbine is a function of the cubed of the wind speed. Thus, the wind speed if doubled, the power produced will be increased by eight times the original power. Then, location of the wind farm plays an important role in order for the wind turbine to extract the most available power form the wind.

The next important factor of the wind turbine is the rotor blade. The rotor blades length of the wind turbine is one of the important aspects of the wind turbine since the power produced from the wind is also proportional to the swept area of the rotor blades i.e. the square of the diameter of the swept area.

$$P_{wind} = \frac{\pi}{8} dD^2 v_{wind}^3$$

Hence, by doubling the diameter of the swept area, the power produced will be four fold increased. It is required for the rotor blades to be strong and light and durable .As the blade length increases, these qualities of the rotor blades become more elusive. But with the recent advances in fiberglass and carbon-fiber technology, the production of lightweight and strong rotor blades between 20 to 30 meters long is possible. Wind turbines with the size of these rotor blades are capable to produce upto 1 megawatt of power the relationship between the power produced by the wind source and the velocity of the wind and the rotor blades swept diameter is shown below.

The derivation to this formula can be looked up in It should be noted that some books derived the formula in terms of the swept area of the rotor blades (A) and the air density is denoted as δ^0.Thus, in selecting wind turbine available in the market, the best and efficient wind turbine is the one that can make the best use of the available kinetic energy of the wind.

3. TYPES OF VSI

3.1 Half-Bride VSI

The power topology of a half-bridge VSI, where two large capacitors are required to provide a neutral point N, such that each capacitor maintains a constant voltage=2. Because the current harmonics injected by the operation of the inverter are low-order harmonics, a set of large capacitors (C. and Cÿ) is required. It is clear that both switches S. and Sÿ cannot be on simultaneously because short circuit across the dc link voltage source Vi would be produced. There are two defined (states 1 and 2) and one undefined (state 3) switch state as shown in Table In order to avoid the short circuit across the dc bus and the undefined ac output voltage condition, the modulating technique should always ensure that at any instant either the top or the bottom switch of the inverter leg is on. Shows the ideal waveforms associated with the half-bridge inverter shown in Fig. The states for the switches S. and Sÿ are defined by the modulating technique, which in this case is a carrier-based PWM.

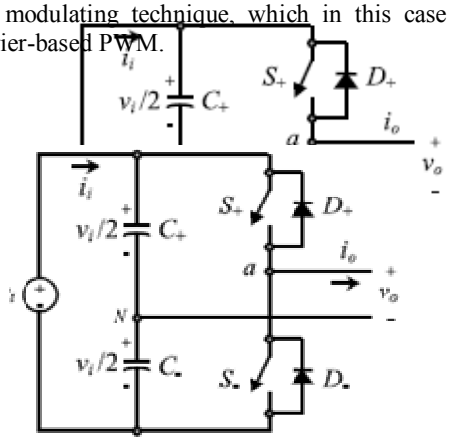

International Journal of Research
Available at https://edupediapublications.org/journals
p-ISSN: 2348-6848
e-ISSN: 2348-795X
Volume 03 Issue 14
October 2016

Fig 3.1: Single phase full Bridge VSI

The Carrier-Based Pulse width Modulation (PWM) Technique: As mentioned earlier, it is desired that the ac output voltage. Va N follow a given waveform (e.g., sinusoidal) on a continuous basis by properly switching the power valves. The carrier-based PWM technique fulfils such a requirement as it defines the on and off states of the switches of one leg of a VSI by comparing a modulating signal Vc (desired ac output voltage) and a triangular waveform V_D (carrier signal). In practice, when Vc > V_D the switch S. is on and the switch is off; similarly, when Vc < V_D the switch S. is off and the switch Sÿ is on. A special case is when the modulating signal Vc is a sinusoidal at frequency fc and amplitude Vc, and the triangular signal V_D is at frequency V_D and amplitude VD. This is the sinusoidal PWM (SPWM) scheme. In this case, the modulation index ma (also known as the amplitude-modulation ratio) the amplitude of the fundamental component of the ac output voltage V_{o1} satisfying the following expression for odd values of the normalized carrier frequency o_f the harmonics in the ac output voltage appear at normalized frequencies f_h centered around mf and its multiples, specifically,

The PWM technique allows an AC output voltage to be generated that tracks a given modulating signal. A special case is the SPWM technique (the modulating signal is a sinusoidal) that provides in the linear region an AC output voltage that varies linearly as a function of the modulation index and the harmonics

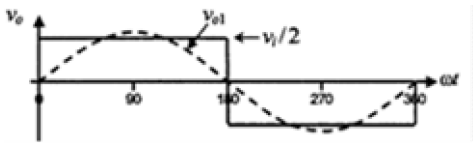

are at well-defined frequencies and amplitudes.

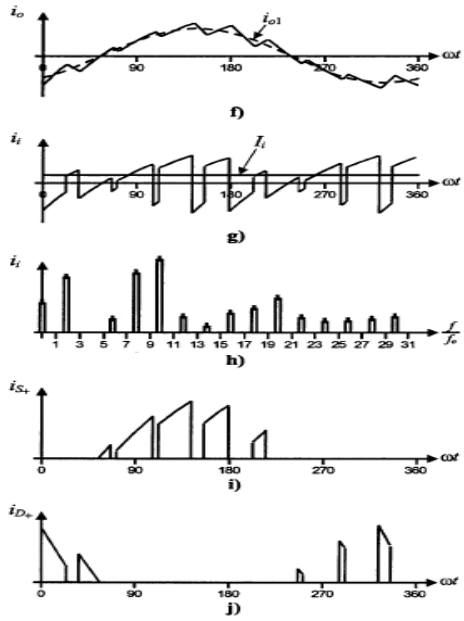

These features simplify the design of filtering components. Unfortunately, the maximum amplitude of the fundamental ac voltage is v_i=2 in this operating mode. Higher voltages are obtained by using the over modulation region (ma > 1); however, low-order harmonics appear in the ac output voltage.

3.2 Full-Bride VSI

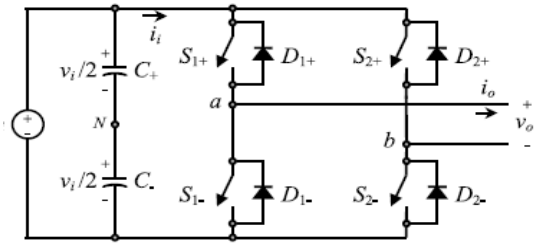

The power topology of a full-bridge VSI. This inverter is similar to the half-bridge inverter; however, a second leg provides the neutral point to the load. As expected, both switches S1 and S1ÿ (or S2. and S2ÿ) cannot be on simultaneously because a short circuit across the dc link voltage source v_i would be produced. There are four defined and one undefined

The undefined condition should be avoided so as to be always capable of defining the ac output voltage. In order to avoid the short circuit across the dc bus and the undefined ac output voltage condition, the modulating technique should ensure that either the top or the bottom switch of each leg is on at any instant. It can be observed that the ac output voltage can take values up to the dc link value Vi which is twice that obtained with half-bridge VSI topologies. Several modulating techniques have been developed that are applicable to full-bridge VSIs. Among them are the PWM (bipolar and unipolar) techniques.

4. Fuzzy Logic Controller

Most of the real-world processes that require automatic control are non-linear in nature. That is, their parameter values alter as the operating point changes over time or both. In case of conventional control schemes, as they are linear, a controller can only be tuned to give good performance at a particular operating point or for a limited period of time. The controller needs to be retuned if the operating point changes with time. This necessity to retune has driven the need for adaptive controllers that can automatically retune themselves to match the current process characteristics.

Fuzzy logic is an innovative technology that enhances conventional system design with engineering expertise. Using fuzzy logic, we can

circumvent the need for rigorous mathematical modeling

Professor Lotfi A Zadeh introduced the concept of fuzzy sets, according to him. Fuzzy logic is a mathematical imprecise description.

The basic configuration of Fuzzy logic control based as shown in Fig. 5.1 consists of four main parts i.e.

(i) Fuzzification,

(ii) Knowledge base,

(iii) Inference Engine and

(iv) Defuzzification.

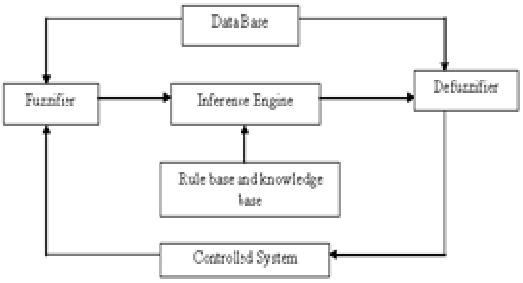

4.1 Fuzzification

Fuzzification maps from the crisp input space to fuzzy sets in certain, input universe of discourse. So for a specific input value x, it is mapped to the degree of membership $\mu_A(x)$. The Fuzzification involves the following functions. Measures the value of input variables.

Flux Error	Torque error / Flux angle	Small	Medium	Large
Negative dλ=0	Small	Small	Small	Medium
	Medium	Small	Medium	Large
	Large	Small	Medium	Large
Positive dλ=1	Small	Small	Medium	Large
	Medium	Small	Medium	Large
	Large	Medium	Large	Large

Table 4.1 fuzzy rules

The inputs and the output of the fuzzy controller are assigned Gausian membership functions as shown in Figs. 4.2. 4.3, 4.4.The universe of discourse for the torque error and the duty ratio is adjusted using simulations to get optimal torque ripple reduction. Since there are three membership functions for each input, it follows that there are nine rules in each set of fuzzy rules. The presented fuzzy controller is for both forward and backward rotation, for backward rotation the absolute value of the torque error is used, and the flux position calculation is adjusted according to the rotation direction.

If (torque error is medium) and (flux position is small) then (duty ratio is small) If (torque error is large) and (flux position is small) then (duty ratio is medium) Using the above reasoning and simulation to find the fuzzy rules, the two sets of fuzzy rules are summarized in Table 4.1.

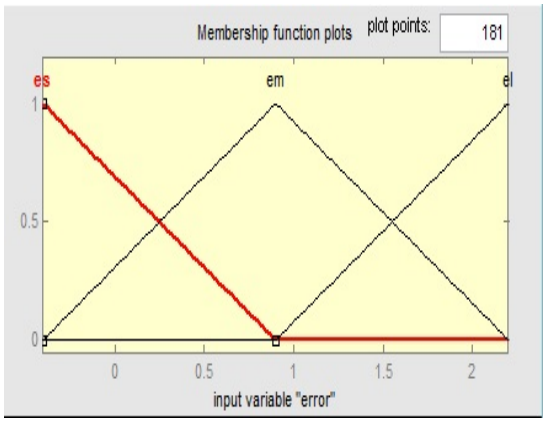

Fig. 4.2 Membership functions distribution for the torque error (input)

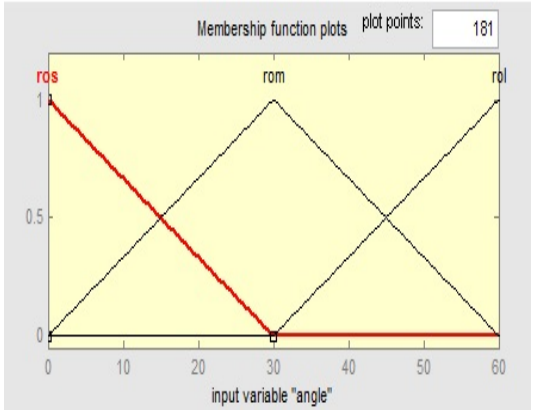

Fig. 4.3 Membership functions distribution for the torque angle(input)

International Journal of Research
Available at https://edupediapublications.org/journals
p-ISSN: 2348-6848
e-ISSN: 2348-795X
Volume 03 Issue 14
October 2016

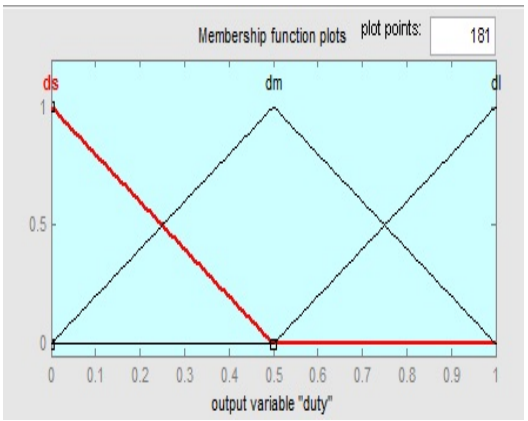

Fig. 4.4 Membership functions distribution for the duty cycle (output)

4.2 Knowledge Base

Table 4.1 shows rule base of the FLC .Max–Min and Max-Dot are planned within the literature of several composition methods. Throughout this paper Min methodology is used. The minimum operator

Knowledge base comprises of the definitions of fuzzy MFs for the input and output variables and the necessary control rules, which specify the control action by using linguistic terms.

4.3 Defuzzification

Defuzzification covers the linguistic variables to determine numerical values. Centroid method of defuzzification is used in this study.

(1) A scale mapping, which converts the range of values of input variables into corresponding universe of discourse.

(2) Defuzzification, which yields a non-fuzzy control action from an inferred fuzzy control action.

5. Grid-side inverter model and control strategy

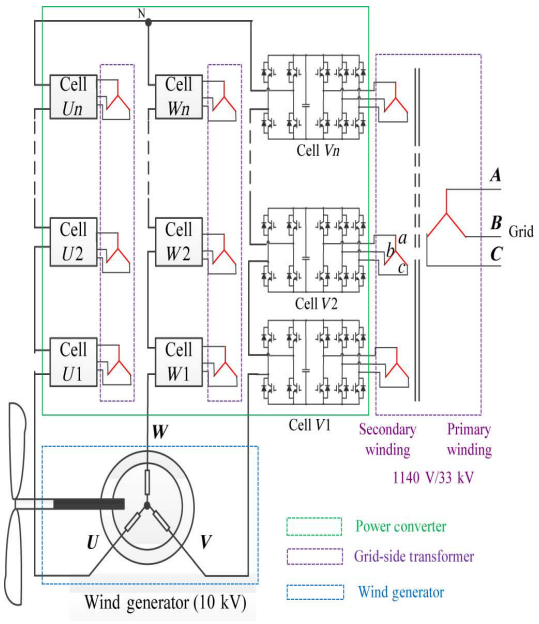

Fig 5. High-power, medium-voltage (10 kV) modular wind converter with grid-side transformer isolation (converter type III) generator and converter structure.

The dynamic model of the grid connection when selecting are reference frame rotating synchronously with the grid voltage space vector is

$$u_d = u_{id} - Ri_d - L\frac{di_d}{dt} + \omega Li_q$$

$$u_q = u_{iq} - Ri_q - L\frac{di_q}{dt} - \omega Li_d$$

(1)

where *L* and *R* are the grid inductance and resistance, respectively, and *uid* and *uiq* are the inverter voltage components. If the reference frame is oriented along the supply voltage, the grid voltage vector is

$$u = u_d + j0$$

(2)

Then active and reactive power may be expressed as

International Journal of Research
Available at https://edupediapublications.org/journals
p-ISSN: 2348-6848
e-ISSN: 2348-795X
Volume 03 Issue 14
October 2016

$$P = \frac{3}{2} u_d i_d$$

$$Q = \frac{3}{2} u_d i_q$$

(3)

Active and reactive power control can be achieved by controlling direct and quadrature current components, respectively. The control of this converter is quite similar to that of the generator. Two control loops are used to control the active and reactive power, respectively [3] (Fig. 5.1).

An outer dc voltage control loop is used to set the *d*-axis current reference for active power control. This assures that all the power coming from the rectifier is instantaneously transferred to the grid by the inverter

The grid-side three-phase inverter control diagram is shown in Fig. 5.1. The outer loop is the dc-link voltage control loop which is kept to be 1800 V and inner loops are -axis and -axis current control loops. The -axis current can be used to provide reactive power to the grid when required subject to the current capability of the converter.

5.1 Resonant Controller Added in the Control Loop

One particular issue with the converter topology shown in Fig. 4 is the large dc-link capacitor required in each cell to smooth the single-phase pulsating power from the H-bridge (generator) side, which can be expressed as

$$p_{g\_single}(t) = v_{o,U}(t) \cdot i_{o,U}(t) = V_{om}\cos(\omega_o t) \cdot I_{om}\cos(\omega_o t - \varphi)$$

$$= \frac{V_{om} I_{om}}{2}\cos\varphi + \frac{V_{om} I_{om}}{2}\cos(2\omega_o t - \varphi)$$

$$= P_{\text{avg}} \cdot \cos\varphi + P_{\text{avg}} \cdot \cos(2\omega_o t - \varphi)$$

(4)

Where V_{om} and I_{om} are the amplitudes of the generator voltage ($V_{o,u}$) and current ($i_{o,u}$)seen at each cell, respectively. P_{avg} is the average power flowing into the converter cell. ω_o is the generator stator frequency and φ is the generator power factor angle. As seen, the second term in (3) represents the pulsating power with the frequency of, 2ω0 which causes dc-link voltage ripple. The amplitude of dc-link voltage ripple ΔV can be expressed as

$$\Delta V = \frac{P_{\text{avg}}}{\omega_o \cdot C \cdot V_{\text{dc}}}$$

(5)

For a 10-MW wind power converter with 15 cells (5 stages), 1800-V dc-link voltage, and 15-Hz generator stator frequency, the required capacitor in each cell will be 44 mF in order to keep the voltage ripple to be within 5% (90 V) at the rated operating point.

To achieve such large capacitance at this voltage level, many electrolytic capacitors need to be connected in both series and in parallel, which are not only expensive and bulky, but also cause reliability issues of the system, since the electrolytic capacitor has almost the highest failure rates in a typical wind power converter system For offshore applications, high reliability is a key to reduce the maintenance cost. Therefore, an effective method to reduce the required dc-link capacitor is critical. Due to the use of controlled three-phase inverter in each cell, the power transferred to the transformer secondary winding can be well adjusted to compensate the power ripple from the H-bridge rectifier. If the power of the three-phase inverter in (3) is regulated the same as the power from the H-bridge rectifier as(4) (including the pulsating power), in theory, no dc-link capacitor is required to handle the low-frequency ($2\omega o$) power ripple.

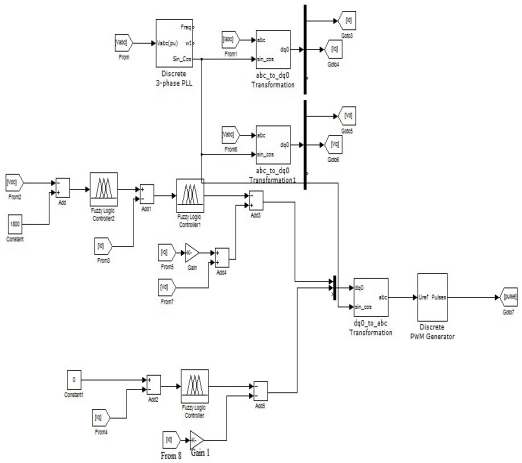

Fig 5.1 simulink block diagram of the grid-side inverter in each cell (The PI controller is replaced with fuzzy controller when the dc-link voltage ripple reduction function is enabled.).

6. SIMULATION ANALYSIS

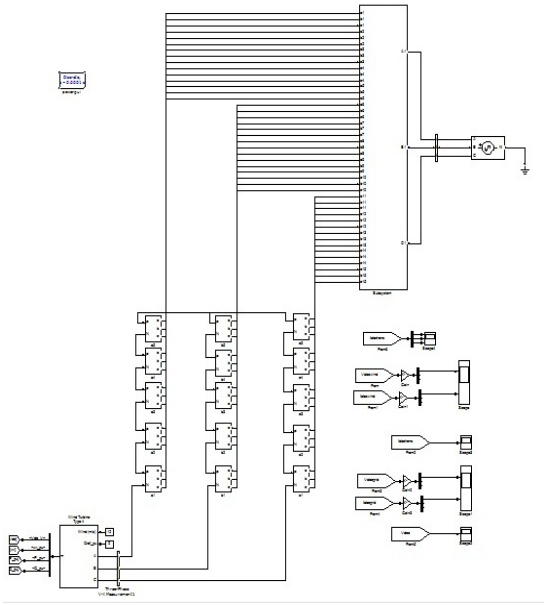

Fig 6.1: Simulation model for constant wind speed by using Fuzzy Controller

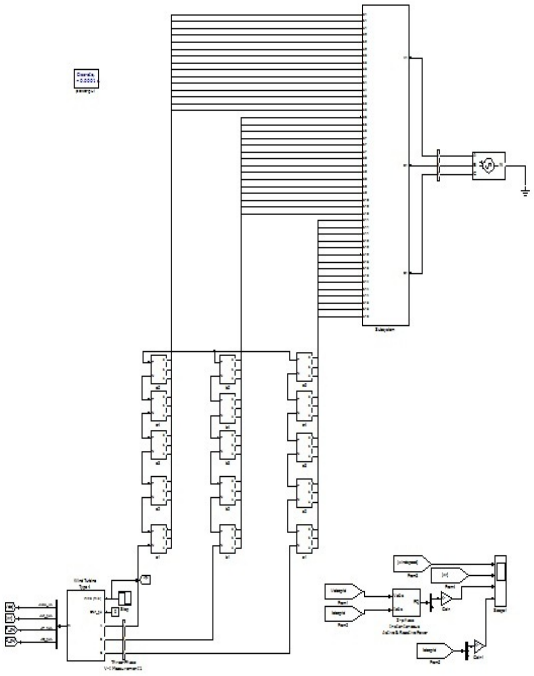

Fig-6.2: Overall Simulink control block for the variable wind speed using fuzzy controller

6.1 Inverter and Transformer Power Losses Analysis

While the low-frequency power ripple from H-bridge side can be effectively compensated from the transformer-side inverter, the harmonic current may cause extra thermal stress to the inverter power devices and the transformer secondary windings. Fig. 7 shows the simulated inverter current waveform with and without the dc-link voltage ripple reduction method applied for a 10-MW system at a rated wind speed. As seen, with the dc-link ripple reduction method applied, the peak current (due to the harmonics) of each phase may double the value of the current without compensation. The exact expression of the current waveform is given in for phase a. Therefore, the power device current rating should be chosen to meet the peak current requirement

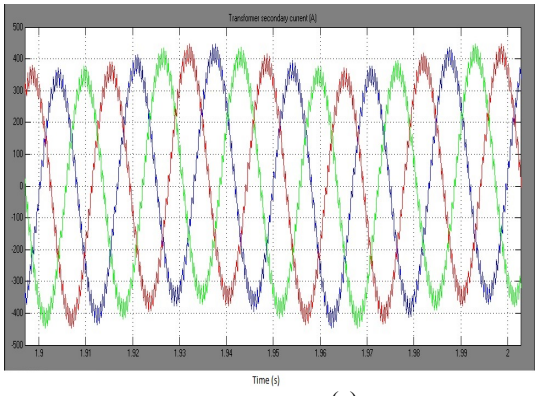

(a)

International Journal of Research
Available at https://edupediapublications.org/journals
p-ISSN: 2348-6848
e-ISSN: 2348-795X
Volume 03 Issue 14
October 2016

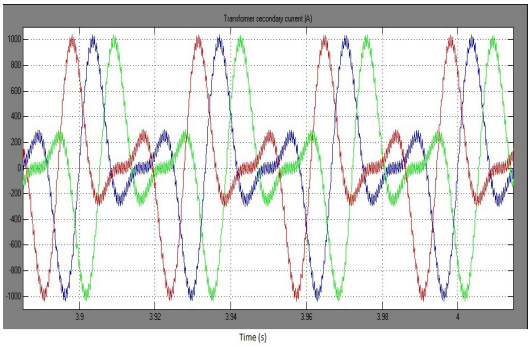

(b)

Fig. 7 Inverter (transformer secondary) current with and without resonant controller applied: (a) without resonant controller and (b) with fuzzy controller

In order to evaluate the thermal performance and the impact of the control algorithm on the inverter, the inverter losses and device junction temperature are calculated and simulated. For a 10-MW, 10-kV generator, the rated root mean square (RMS)current is 577 A. With a 1140-V/33-kV grid-side transformer and15 converter cells, the transformer secondary winding RMS current is 337 A. Note that if the ripple power compensation scheme is activated, the peak of transformer secondary current may increase to 950 A.

6.2 SIMULATION RESULTS

A. Case 1: Steady-state simulation results at the wind speed of 12 m/s with 10-MW wind power generation.

Fig. 8(a) shows the generator-side converter output voltage, which has 11 levels and the generator current. Fig. 8(b)shows the transformer secondary winding (inverter) currents(1140-V side) in one converter cell

The grid (33 kV) phase voltage and current are shown in Fig. 8(c). As seen, the grid current is kept sinusoidal and the phase relationship between voltage and current indicates wind power is fed into the grid.

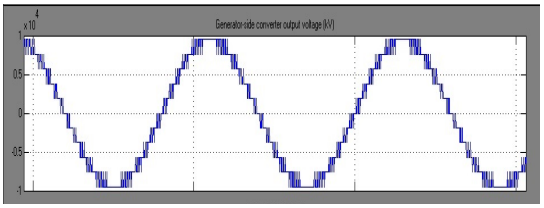

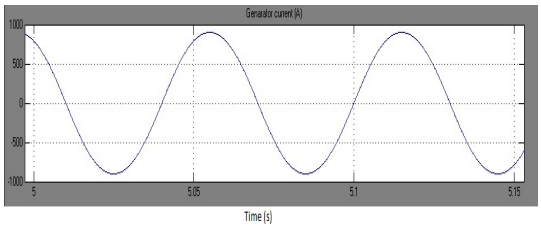

(a)

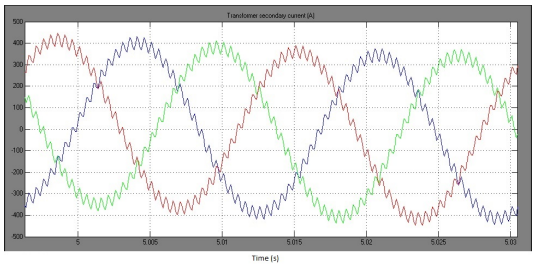

(b)

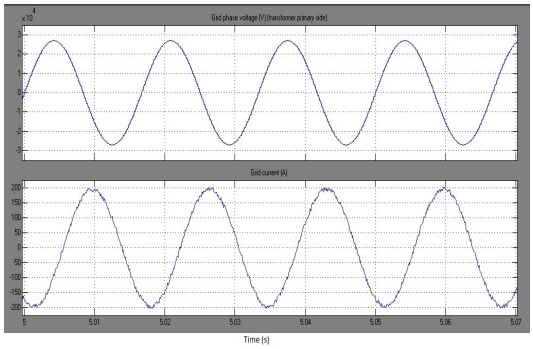

(c)

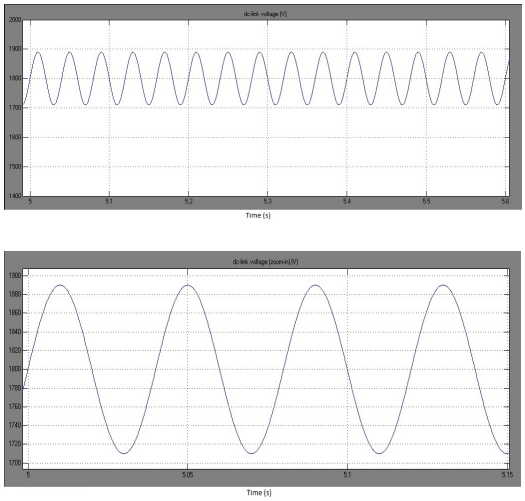

(d)

Fig 8.Steady-state simulation results at wind speed of 12 m/s: (a) generator side converter output voltage and generator current, (b) transformer secondary winding current in a converter cell, (c) grid phase voltage and current, and (d) dc-link voltage and detailed trace.

Fig. 8(d) shows the dc-link voltage regulated at 1800 V. With 44-mF dc-link capacitor, the voltage ripple is around 90 V, which agrees with the calculated results by (5). A detailed waveform is shown at the bottom of this figure and the ripple frequency is 30 Hz, which is twice of the generator frequency of 15 Hz.

B. Case 2: System response during wind speed drop from 12 to 10 m/s.

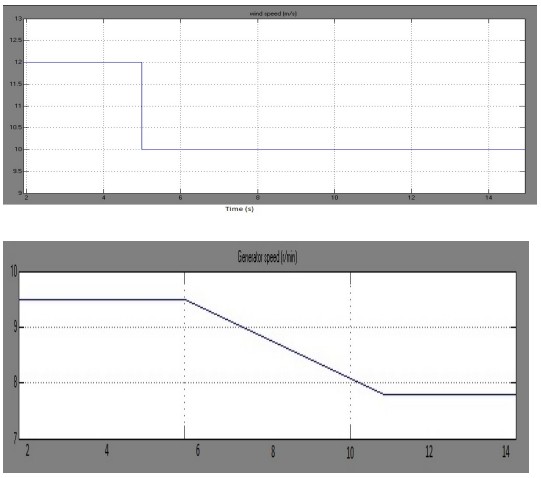

(a)

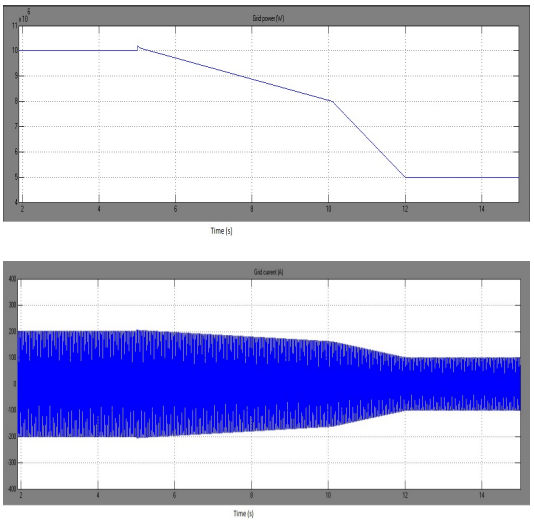

(b)

Fig. 9. System response during wind speed drop from 12 to 10 m/s: (a) wind speed and generator speed and (b) power transferred to the grid and grid current

Fig. 9 shows the system response during a wind speed drop from 12 to 10 m/s at 5 s. The converter and generator control aims to achieve MPPT under both wind speeds.

Fig. 9(a) shows the wind speed profile and the corresponding generator speed. As seen, the generator speed reduces from 9.5 (MPPT point for 12 m/s) to 7.7 r/min to reach the MPPT point. Fig. 9(b) shows the power transferred to the grid and the grid current.

C. Case 3: Simulation results with a FUZZY controller.

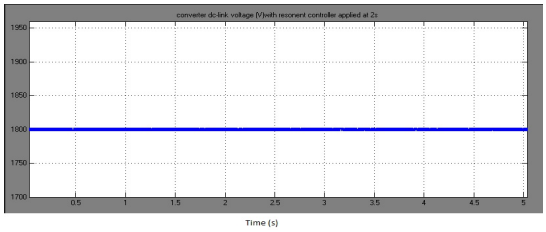

(a)

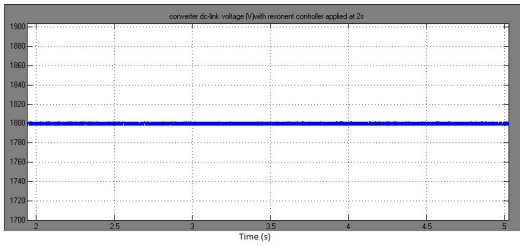

(b)

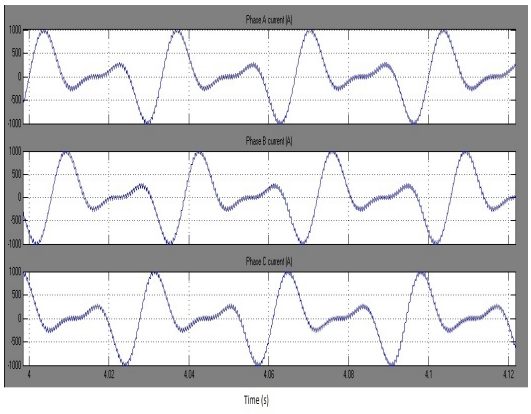

(c)

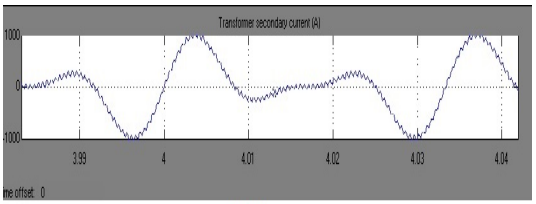

(d)

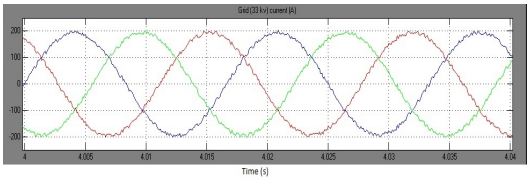

(e)

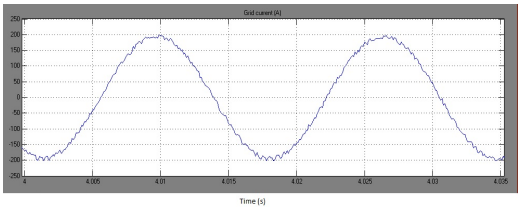

(f)

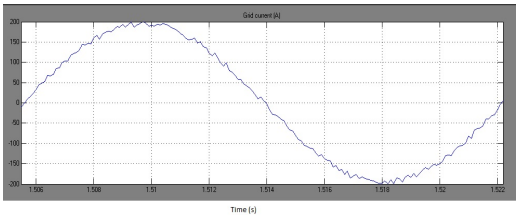

(g)

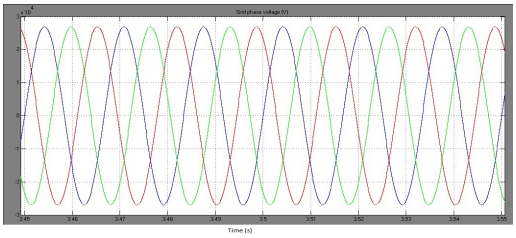

(h)

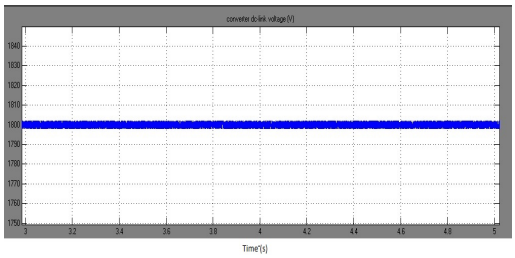

(i)

Fig. 10 : Simulation results with a FUZZY controller engaged to reduce the dc-link voltage ripple: (a) converter cell dc-link voltage with resonant controller applied at 2 s, (b) dc-link voltage during generator speed variation, (c) transformer secondary winding current, (d) FFT analysis of transformer secondary winding current, (e) transformer primary (grid) current, (f) FFT analysis of transformer primary winding current, (g) THD of the grid current, (h) grid phase voltages with phase 10% drop at 3.5 s, and (i) converter dc-link voltage under unbalanced grid.

Fig. 10 shows the results of dc-link voltage ripple reduction by using the FUZZY controller in the dc-link voltage and current control loops of each converter cell, as illustrated in the diagram in Fig. 5.1 To observe the effect more clearly, the dc-link capacitance has been reduced from 44 to 22 mF. Therefore, without using FUZZY controller, the dc-link voltage ripple of each cell should be 180 V. Fig. 10(a) shows the dc link voltage, where the resonant controller is applied at 2 s.

Fig 10(c) shows the result of corresponding transformer secondary current in each cell when the resonant controller is engaged. As seen, the currents are not sinusoidal due to the compensation of the pulsation power. The fast Fourier transform (FFT) analysis of the current is shown in Fig. 10(d).Fig. 10(e) shows the transformer primary (grid)-side current waveform, which is sinusoidal and does not contain any low-frequency harmonics as indicated by the FFT analysis in Fig. 10(f) that only the 60-Hz grid-frequency component appears. It is evident that the proposed dc-link voltage ripple reduction method does not affect the grid-side power quality. Fig. 10(g) shows the total harmonic distortion (THD) of the grid current, which is 4.52% in this case, where the grid-interface inductance is 0.5 mH and the switching frequency is 2 kHz. Fig. 10(h) and (i) shows the effectiveness of the dc-link voltage ripple reduction scheme under an unbalanced grid condition. At 3.5 s, phase voltage has a 10% voltage drop. From the converter dc-link voltage, it can be

seen that the dc-link voltage ripple is effectively attenuated regardless the voltage drop in phase.

7. CONCLUSIONS

In this paper, three high-power medium-voltage (10 kV) modular wind power converter topologies have been derived based on a generalized structure by using different formats of isolation. A method has been proposed to attenuate the dc-link voltage ripple, thus reducing the capacitor requirement, by compensating the low-frequency power ripple. A Fuzzy controller-based control loop has been designed to achieve this purpose. The proposed dc-link voltage reduction scheme will introduce harmonics in the transformer secondary current; however, not degrading the grid power quality (sinusoidal current). The current harmonics will increase the stress of the power devices and the transformer copper loss. Simulation results with a 10-kV, 10-MW system have validated the converter topology and control scheme. The proposed dc-link voltage ripple reduction method may also be used in the other two topologies presented in the paper.

REFERENCES

[1] M.Liserre, R.Cardenas, M.Molinas, andJ.Rodriguez, "OverviewofmultiMW wind turbines and wind parks," IEEE Trans. Ind. Electron., vol. 58, no. 4, pp. 1081–1095, Apr. 2011.

[2] F.Blaabjerg,M.Liserre,andK. Ma,"Power electronics converters forwind turbine systems," IEEE Trans. Ind. Appl., vol. 48, no. 2, pp. 708–719, Mar. 2012.

[3] M. Chinchilla, S. Arnaltes, and J. Burgos, "Control of permanent-magnet generators applied to variable-speed wind-energy systems connected to the grid,IEEETrans.EnergyConvers" vol.21,no.1,pp.130–135,Mar.2006.

[4] J. Dai, D. Xu, and B. Wu, "A novel control scheme for current–source– converter-based PMSG wind energy conversion systems," IEEE Trans. Power Electron., vol. 24, no. 4, pp. 963–972, Apr. 2009.

[5] J. Birk and B. Andresen, "Parallel-connected converters for optimizing efficiency, reliability and grid harmonics in a wind turbine," in Proc. EPE'07 Conf., Aalborg, Denmark, Sep. 2007, pp. 1–7.

[6] Z. Xu, R. Li, H. Zhu, D. Xu, and C. H. Zhang, "Control of parallel multiple converters for direct-drive permanent-magnet wind power generation systems," IEEE Trans. Power Electron., vol. 27, no. 3, pp. 1250–1270, Mar. 2012.

[7] W. Erdman and M. Behnke, "Low wind speed turbine project phase II: The application of medium-voltage electrical apparatus to the class of variable speed multi-megawatt low wind speed turbines," San Ramon, CA, USA, Natl. Renew. Energy Lab. Rep., NREL/SR-500-38686, Nov. 2005.

[8] H. Abu-Rub, J. Holtz, J. Rodriguez, and G. Baoming, "Medium-voltage multilevel converters-state of the art, challenges and requirements in industrial applications," IEEE Trans. Ind. Electron., vol. 57, no. 8, pp. 2581–2596, Aug. 2010.

[9] R. C. Portillo, M. M. Prats, J. I. Leon, J. A. Sanchez, J. M. Carrasco, E. Galvan et al., "Modelling strategy for back-to-back three-level converters applied to high-power wind turbines," IEEE Trans. Ind. Electron., vol. 53, no. 5, pp. 1483–1491, Oct. 2006.

[10] E. J. Bueno, S. Cóbreces, F. J. Rodríguez, A. Hernández, and F. Espinosa, "Design of a back-to-back NPC converter interface for wind turbines with squirrel-cage induction generator," IEEE Trans. Energy Convers., vol. 23, no. 3, pp. 932–945, Sep. 2008.

[11] A. Faulstich, J. K. Steinke, and F. Wittwer, "Medium voltage converter for permanent magnet wind power generators up to 7 MW," in Proc. EPE Conf., Barcelona, Spain, Sep. 2009, pp. 9–17.

[12] C. L. Xia, X. Gu, and Y. Yan, "Neutral-point potential balancing of threelevel inverters in direct-driven wind energy conversion system," IEEE Trans. Energy Convers., vol. 26, no. 1, pp. 18–29, Mar. 2011.

[13] M. Winkelnkemper, F. Wildner, and P. K. Steimer, "6 MVA five-level hybrid converter for wind power," in Proc. IEEE PESC'08 Conf., Rhodes, Greece, Jun. 2008, pp. 4532–4538.

[14] X. Yuan, J. Chai, and Y. Li, "A transformer-less high-power converter for large permanent magnet wind generator systems," IEEE Trans. Sustain. Energy, vol. 3, no. 3, pp. 318–329, Jul. 2012.

[15] C. Xia, Z. Wang, T. Shi, and Z. Song, "A novel cascaded boost chopper for the wind energy conversion system based on the permanent magnet synchronous generator," IEEE Trans. Energy Convers., vol. 28, no. 3, pp. 512–522, Sep. 2013.

[16] C. H. Ng, M. A. Parker, R. Li, P. J. Tavner, J. R. Bumby, and E. Spooner, "A multilevelmodularconverterfor alargelightweightwindturbinegenerator," IEEE Trans. Power Electron., vol. 23, no. 3, pp. 1062–1074, May 2008.

[17] M. A. Parker, C. H. Ng, and L. Ran, "Fault-tolerant control for a modular generator converter scheme for direct drive wind turbines," IEEE Trans. Ind. Electron., vol. 58, no. 1, pp. 305–315, Jan. 2011.

[18] J. Kang, N. Takada, E. Yamamoto, and E. Watanabe, "High power matrix converter for wind power generation applications," in Proc. ICPE ECCE Asia Conf., Jeju, Korea, Jun. 2011, pp. 1331–1336.

[19] M. A. Perez, J. R. Espinoza, J. R. Rodriguez, and P. Lezana, "Regenerative medium voltage AC drive based on a multicell arrangement with reduced energy storage requirements," IEEE Trans. Ind. Electron., vol. 52, no. 1, pp. 171–180, Feb. 2005.

[20] S. Inoue and H. Akagi, "A bidirectional isolated dc–dc converter as a core circuit of the next-generation medium-voltage power conversion system," IEEE Trans. Power Electron., vol. 22, no. 2, pp. 535–542, Mar. 2007.

[21] F. Iov, F. Blaabjerg, J. Clare, O. Wheeler, A. Rufer, and A. Hyde, "UNIFLEX-PM-A key-enabling technology for future European electricity networks," EPE J., vol. 19, no. 4, pp. 6–16, 2009.

[22] J. Rodriguez, S. Bernet, B. Wu, J. O. Pontt, and S. Kouro, "Multilevel voltage source converter topologies for industrial medium-voltage drives," IEEE Trans. Ind. Electron., vol. 54, no. 6, pp. 2930–2945, Dec. 2007.

[23] H.D.Bang,R.P.Roojj,A.S.McDonald,andM.A.Mueller,"10M Wwind turbinedirectdrivegeneratordesignwithpitchoractivespeedstall control," in Proc. IEEE IEMDC Conf., Antalya, Turkey, vol. 2, May 2007, pp. 1390–1395.

[24] X. Yuan, F. Wang, D. Borojevich, Y. Li, and R. Burgos, "Dc-link voltage control of a full power converter for wind generator operating in weak-grid systems," IEEE Trans. Power Electron., vol. 24, no. 9, pp. 2178–2192, Sep. 2009.

[25] R. Cardenas and R. Pena, "Sensorless vector control of induction machines for variable-speed wind energy applications," IEEE Trans. Energy Convers., vol. 19, no. 1, pp. 196–205, Mar. 2004.

[26] P. J. Tavner, G. J. W. Bussel, and F. Spinato, "Machine and converter reliabilities in wind turbines," in Proc. IET PEMD'06 Conf., Dublin, Ireland, Mar. 2006, pp. 127–130.
[27] R. Teodorescu, F. Blaabjerg, M. Liserre, and P. C. Loh, "Proportionalresonant controllers and filters for grid-connected voltage–source converters," IEE Proc. Elect. Power Appl., vol. 153, no. 5, pp. 750–762, Sep. 2006.
[28] R. Teodorescu, M. Liserre, and P. Rodriguez, Grid Converters for Photovoltaic and Wind Power Systems, Chap. 4. Hoboken, NJ, USA: Wiley, 2011.
[29] IGBT module datasheet [Online]. Available: http://www.infineon.com/ dgdl

Student Details:

Mr. PELLETI SIVARAMAIAH was born in India.He pursuing M.Tech degree in Power Systems EEE Department in N.B.K.R. Institute of Science and Technology ,S.P.S.R Nellore, Andhra Pradesh State ,India.

mail id: siva6rise@gmail.com

Guide Details:

Smt.Panneerselvam Dhana Selvi was born in India. She received B.Tech degree in Electrical and Electronics Engineering from Periyar University & M.E degree in Electrical power engineering from JNTUH. Her research interests are in the area of power systems especially Optimal tuning of power system stabilizer parameters using genetic algorithm.

Email id:dhanaselvi.nbkrist@gmail.com